REGULAR ARTICLE

blood advances

Medullary stromal cells synergize their production and capture of CCL21 for T-cell emigration from neonatal mouse thymus

Kieran D. James,[1] Daniel F. Legler,[2,3] Vladimir Purvanov,[3] Izumi Ohigashi,[4] Yousuke Takahama,[5] Sonia M. Parnell,[1] Andrea J. White,[1] William E. Jenkinson,[1] and Graham Anderson[1]

[1]Institute of Immunology and Immunotherapy, University of Birmingham, Birmingham, United Kingdom; [2]Biotechnology Institute Thurgau, University of Konstanz, Kreuzlingen, Switzerland; [3]Faculty of Medicine, University of Bern, Bern, Switzerland; [4]Division of Experimental Immunology, Institute of Advanced Medical Sciences, Tokushima University, Tokushima, Japan; and [5]Experimental Immunology Branch, National Cancer Institute, National Institutes of Health, Bethesda, MD

Key Points

- We report an important, nonredundant role for the chemokine CCL21 in controlling emigration of αβT cells from the neonatal thymus.
- Medullary epithelium and mesenchyme function together to produce and capture CCL21 and focus its accumulation at sites of thymic exit.

The release of newly selected αβT cells from the thymus is key in establishing a functional adaptive immune system. Emigration of the first cohorts of αβT cells produced during the neonatal period is of particular importance, because it initiates formation of the peripheral αβT-cell pool and provides immune protection early in life. Despite this, the cellular and molecular mechanisms of thymus emigration are poorly understood. We examined the involvement of diverse stromal subsets and individual chemokine ligands in this process. First, we demonstrated functional dichotomy in the requirement for CCR7 ligands and identified CCL21, but not CCL19, as an important regulator of neonatal thymus emigration. To explain this ligand-specific requirement, we examined sites of CCL21 production and action and found *Ccl21* gene expression and CCL21 protein distribution occurred within anatomically distinct thymic areas. Although *Ccl21* transcription was limited to subsets of medullary epithelium, CCL21 protein was captured by mesenchymal stroma consisting of integrin $\alpha7^+$ pericytes and $CD34^+$ adventitial cells at sites of thymic exit. This chemokine compartmentalization involved the heparan sulfate–dependent presentation of CCL21 via its C-terminal extension, explaining the absence of a requirement for CCL19, which lacks this domain and failed to be captured by thymic stroma. Collectively, we identified an important role for CCL21 in neonatal thymus emigration, revealing the importance of this chemokine in initial formation of the peripheral immune system. Moreover, we identified an intrathymic mechanism involving cell-specific production and presentation of CCL21, which demonstrated a functional synergy between thymic epithelial and mesenchymal cells for αβT-cell emigration.

Introduction

Intrathymic development of conventional single-positive (SP) $CD4^+$ and $CD8^+$ αβT-cell receptor (αβTCR)–expressing αβT cells involves maturation events that occur within cortical and medullary microenvironments. Although this program ensures the generation of functionally competent self-tolerant thymocytes, additional postselection maturation events are required to establish T cell–mediated immunity.[1-3] Of particular importance is thymus emigration, where mature T cells are released into peripheral tissues.[4-7] The importance of this process is perhaps most evident during the neonatal period, where emigration of conventional SP thymocytes establishes the peripheral T-cell pool.[8,9] Indeed, the essential requirement for neonatal thymus emigration is clear from long-standing observations in which disrupted formation of the peripheral T-cell pool via neonatal thymectomy

Submitted 14 August 2020; accepted 31 October 2020; published online 5 January 2021. DOI 10.1182/bloodadvances.2020003192.

For original data requests, please contact k.d.j.james@bham.ac.uk.

The full-text version of this article contains a data supplement.

results in systemic autoimmunity, caused by the early emigration of effector T cells and the delayed emigration of Foxp3$^+$ regulatory T cells.[10-12]

Medulla-resident CD62L$^+$CD69$^-$ SP thymocytes represent egress-competent cells,[13,14] and evidence suggests the presence of a conveyor-belt process, which biases export toward the most mature cells.[15] Also, SP thymocytes within perivascular spaces at the corticomedullary junction (CMJ) have identified potential sites of thymic exit.[16] In terms of molecular regulation, the sphingosine-1-phosphate (S1P) receptor $S1P_1$ controls late stages of thymus emigration, allowing mature SP thymocytes near thymic blood vessels to undergo reverse transendothelial migration and enter the circulation.[17,18] Despite this, mechanisms controlling the trafficking of mature thymocytes through the medulla and toward sites associated with S1P-dependent emigration are poorly understood. This may be due to difficulties in directly attributing alterations in thymocyte populations to defects in thymus emigration. For example, increased SP thymocytes in neonatal *Ccr7*$^{-/-}$ and CCR7 ligand (CCR7L)–deficient *plt*/*plt* mice[9,19] could be due to defective emigration, enhanced thymocyte proliferation,[20] and/or failures in negative selection.[21,22] As such, other than $S1P_1$, the importance of thymocyte-expressed regulators of neonatal thymus emigration are unclear.

Here, we studied the requirement for CCR7Ls CCL19 and CCL21 in neonatal thymus emigration. From analysis of *plt*/*plt*Rag2GFP mice, where *green fluorescent protein* (GFP) indicated cellular age and medullary dwell time,[13,23,24] we showed CCR7/CCR7L controlled neonatal thymic exit. Furthermore, comparative analysis of *Ccl19*$^{-/-}$ and *Ccl21a*$^{-/-}$ neonates demonstrated an important requirement for CCL21, but not CCL19, in this process. Finally, we showed CCL21 production by medullary thymic epithelial cells (mTECs) was coupled with heparan sulfate–dependent presentation by mesenchymal adventitial cells and pericytes, enabling CCL21 to accumulate at sites of thymic exit. Collectively, we identified the importance of CCL21 in the control of neonatal thymus emigration and revealed a mechanism where mTEC/mesenchyme synergy ensured its production and presentation at sites of thymic exit.

Materials and methods

Mice

Neonatal mice were used at age 10 days: wild-type (WT) C57BL/6, *plt*/*plt*,[25] *Ccl19*$^{-/-}$,[26] and *Ccl21*^{tdTom} knock-in.[27] Heterozygous *Ccl21*^{tdTom} reporter mice were used to analyze *Ccl21a* expression, and homozygous mice were used as *Ccl21a*-deficient mice alongside heterozygous littermates. CD45.1$^+$BoyJ mice were used at age 8 weeks as hosts for thymus grafting. *plt*/*plt* mice were crossed with Rag2GFP[28] mice to generate *plt*/*plt*Rag2GFP mice. Mice were housed at the Biomedical Services Unit, University of Birmingham. All experiments were approved by the Birmingham Animal Welfare and Ethical Review Board and UK Home Office.

Flow cytometry

For T-cell analysis, tissues were enzymatically digested using collagenase D (2.5 mg/mL; Roche) and DNase I (40 mg/mL; Roche). Spleens were treated with Red Cell Lysis Buffer (Sigma). Suspensions were stained with the following antibodies: anti-CD25 (eBio3C7), anti-TCRβ (H57.597), anti-FoxP3 (FJK-16s), anti-CD69 (H1.2F3), anti-CD62L (MEL-14,), anti-CD45.1 (A20), and anti-CD45.2 (104; eBioscience), as well as anti-CD4 (RM4-5) and anti-CD8 (53-6-7; BioLegend). For stromal analysis, thymus was digested using collagenase dispase (2.5 mg/mL; Roche) and DNase I (40 mg/mL; Roche). CD45$^+$ cells were depleted using anti-CD45 microbeads and LS columns (Miltenyi Biotec). Suspensions were stained with the following: anti-EpCAM1 (G8.8), anti-CD45 (30-F11), anti-CD31 (eBio 390/390), anti-Ly51 (6C3), and anti-IA/IE (M5/114.15.2; eBioscience); LIVE/DEAD Fixable Dead Cell Stain Kit (Invitrogen); anti-CD80 (16-10A1) and anti-TER119 (TER119; BioLegend); UEA1 biotin (Vector Labs) detected using streptavidin phycoerythrin-Cy7 (eBioscience); anti-CD34 biotin (RAM34; eBioscience) detected using streptavidin BV786 (BioLegend); and anti–integrin α7 (334908; R&D Systems). Heparan sulfate was detected using anti–heparan sulfate (10E4; AMSbio) and anti-mouse immunoglobulin M (IgM) fluorescein isothiocyanate (FITC; eB121-15F9; eBioscience). Anti–Δ heparan sulfate (3G10; AMSbio) antibody was used to reveal the neo-epitope (unsaturated uronic acid) exposed on the core protein upon digestion using heparinase III and detected with anti-mouse IgG FITC (eBioscience). Acquisition was performed using an LSR Fortessa (Becton Dickinson), and data were processed using FlowJo (BD Life Sciences).

Confocal microscopy

Sections (7 μm) were cut from snap-frozen thymus tissue and then fixed in acetone. For *Ccl21*^{tdTom} reporter sections, tissues were paraformaldehyde fixed in 2% paraformaldehyde and 30% sucrose. Antibodies/reagents used were as follows: 4′,6-diamidino-2-phenylindole, anti-CD205 (ab51817; Abcam), UEA1 biotin (Vector Labs) detected using streptavidin 555 (Invitrogen), anti-CD31 (WM-59; eBioscience), ERTR5[29] detected using anti-rat IgM 647 (Invitrogen), anti-CCL21 (Lifespan Bioscience) detected using anti-rabbit 647 (Life Technologies), anti–heparan sulfate (10E4; AMSbio) detected using anti-mouse IgM FITC (eB121-15F9; eBioscience), and anti–Δ-heparan sulfate (3G10; AMS Biotechnology) antibody detected with anti-mouse IgG FITC (eBioscience).

Thymus transplantation

Embryonic day–17 thymic lobes were transplanted under the kidney capsule of congenic CD45.1$^+$ C57BL/6 mice.[24] After 7 days, spleen and inguinal lymph nodes were harvested, and graft-derived CD45.2$^+$TCRβ$^+$ T-cells were quantitated.

Stromal presentation of fluorescently tagged chemokines

Cloning and production of CCL19–*monomeric red fluorescent protein* (mRFP) and CCL21-mRFP have been described.[30] To generate a truncated version of CCL21-mRFP lacking the charged C-terminal extension known to account for heparan sulfate binding, we replaced the complementary DNA encoding for the full-length mature CCL21 (amino acids 24-134) with its truncated form (tCCL21; amino acids 24-101) by polymerase chain reaction using the primers CCL21_truncF: 5′-CCA GCC CAG GAA TTC AGG AAG GAC AGG and CCL21_truncR: 5′-CCT GTC CTT CCT GAA TTC CTG GGC TGG TTT C. HEK293 cells were transiently transfected with pHis$_6$-SUMO-tCCL21-mRFP, and the supernatants containing the secreted fluorescently labeled chemokine were collected. His$_6$-SUMO-tCCL21-mRFP proteins were purified over an Ni^{2+} column and digested with SUMOstar

protease (LifeSensors), liberating tCCL21-mRFP with its natural mature N-terminus, which was repurified again over an Ni^{2+} column as described for CCL19-mRFP and CCL21-mRFP.[30] Thymic stromal cells were incubated for 30 minutes at room temperature with 5 nM of fluorescently tagged CCL21, CCL19, or tCCL21, washed, and then stained with cell surface markers to identify individual stromal subsets.

Heparinase III enzyme treatment

Thymus stromal suspensions or sections were incubated for 60 minutes at 37°C with 2 μg/mL of heparinase III (R&D Systems) in 0.1% bovine serum albumin (or 0.1% bovine serum albumin alone for controls), with an additional 100 μL added after 30 minutes. Suspensions were washed and stained with indicated antibodies, and sections were stained with anti-CD31 and anti–heparan sulfate/Δ-heparan sulfate.

Statistical analysis

Graphpad Prism 8 software was used for all analyses. Unpaired 2-tailed Student *t* tests were used unless otherwise stated. Significance is stated in figure legends; nonsignificant differences were not specified.

Results

CCR7L deficiency increases intrathymic dwell time of mature SP thymocytes

To examine how CCR7Ls influence neonatal thymus emigration, we examined thymocytes in CCR7L-deficient *plt*/*plt* mice,[25] using +/*plt* littermate controls to limit interlitter variation. In line with earlier studies,[9] we examined mice at postnatal day 10 to study the first cohorts of αβT cells in both thymus and periphery. Initial analysis showed increased numbers of conventional $CD25^-Foxp3^-TCR\beta^{hi}CD4^+CD8^-$ SP4 (cSP4) and $TCR\beta^{hi}CD4^-CD8^+$ SP8 (SP8) thymocytes in *plt*/*plt* mice (Figure 1A; supplemental Figure 1). Although this agrees with earlier studies,[9] it has not yet been assessed whether this specifically relates to perturbations in thymus emigration and/or other intrathymic events. To address this, we subdivided bulk cSP4 and SP8 thymocytes into immature egress-incompetent ($CD69^+CD62L^-$) and mature egress-competent ($CD69^-CD62L^+$) cells. Strikingly, mature $CD69^-CD62L^+$ subsets of both cSP4 and SP8, but not immature $CD69^+CD62L^-$ subsets, were increased in *plt*/*plt* mice (Figure 1B-C). Thus, *plt*/*plt* mice showed a selective increase in mature thymocytes. Importantly, percentages of $Ki67^+$ mature cSP4 (Figure 1B) or SP8 (Figure 1C) thymocytes in *plt*/*plt* mice were not increased. Rather, $Ki67^+$ mature cSP4 were decreased in *plt*/*plt* mice (Figure 1B). The reasons for this are unknown; however, this argues that increased mature SP thymocytes in *plt*/*plt* mice are not due to increased proliferation. Rather, our findings are consistent with the idea that intrathymic accumulation in the absence of CCR7L is caused by defective emigration.

To investigate this, we crossed *plt*/*plt* mice with Rag2GFP mice,[28] where GFP levels indicated cellular age and length of time SP thymocytes spent in the thymus.[13,14,23] Interestingly, significantly decreased GFP levels were observed in mature $CD69^-CD62L^+$ cSP4 (Figure 1D) and $CD69^-CD62L^+$ SP8 (Figure 1E) from *plt*/*plt* mice. Importantly, proliferation of mature cSP4 and SP8 did not increase (Figure 1B-C), excluding the possibility that reduced GFP is caused by enhanced proliferation-associated GFP dilution. To examine whether *plt*/*plt* SP thymocytes display increased dwell time, we subdivided $CD69^-CD62L^+$ mature cSP4 and SP8 thymocytes into developmental stages[14] based on CD62L levels, where $CD62L^{lo}$ (M2a) are the least mature, followed by $CD62L^{int}$ (M2b) and the most mature $CD62L^{hi}$ (M2c) cells (supplemental Figure 1). Because M2c cells express the highest levels of $S1P_1$ within $CD69^-CD62L^+$ cells and are enriched within recent thymus emigrants (RTEs),[14] their intrathymic frequency indicates thymus emigration rates. We saw a significant bias toward cSP4 and SP8 cell M2c subsets in *plt*/*plt* mice (Figure 1F), which was accompanied by selective reductions in GFP levels in cSP4 and SP8 M2c cells (Figure 1G). Collectively, alterations in mature subsets of cSP4 and SP8 thymocytes in neonatal *plt*/*plt* mice indicate prolonged intrathymic dwell times, providing evidence of a role for CCR7L in thymus emigration.

CCL21 is important for neonatal thymus emigration

plt/*plt* mice carry a genomic deletion resulting in absence of both *Ccl19* and *Ccl21a* loci, the latter encoding the CCL21Serine (CCL21Ser) form of CCL21.[25,31] Therefore, it is not known whether thymus emigration defects in *plt*/*plt* mice are due to absence of individual or multiple CCR7Ls. Because CCL19 and CCL21Ser are both detectable in WT thymus,[32] we examined thymus emigration in neonatal mice lacking either CCL19 ($Ccl19^{-/-}$)[26] or CCL21Ser ($Ccl21a^{-/-}$).[27] Importantly, analysis of SP thymocyte heterogeneity in $Ccl19^{-/-}$ mice showed no alterations in cSP4 and SP8 thymocytes, including mature $CD69^-CD62L^+$ cells (supplemental Figure 2A-C) and their M2a, M2b, and M2c subsets (supplemental Figure 2D). Thus, CCL19 does not play an important role in thymus emigration. In contrast, comparable analysis of $Ccl21a^{-/-}$ neonates showed significantly increased mature $CD69^-CD62L^+$ cSP4 and SP8 thymocytes (Figure 2A-C). Moreover, we saw a selective increase in $CD62L^+$ M2c cells for both cSP4 and SP8 (Figure 2D). Thus, accumulations of egress-competent cSP4 and SP8 thymocytes in *plt*/*plt* mice were observed in $Ccl21a^{-/-}$ but not $Ccl19^{-/-}$ mice, suggesting an important role for CCL21Ser, but not CCL19, in thymus emigration.

As well as causing an accumulation of SP thymocytes, impaired thymus emigration also reduces RTEs in peripheral tissues.[4,33] However, because CCR7Ls control T-cell migration into secondary lymphoid tissues,[25-27,34] alterations in the peripheral T-cell compartments of CCR7/CCR7L-deficient mice cannot be directly attributed to altered thymus emigration. To examine whether accumulation of mature SP thymocytes in $Ccl21a^{-/-}$ mice maps to specific requirements for thymic expression of CCL21Ser, we transplanted $CD45.2^+$ $Ccl21a^{-/-}$ or $CD45.2^+$ $Ccl21a^{+/-}$ lymphoid thymic lobes into WT $CD45.1^+$ mice (Figure 3A). Here, we were able to track emigration of a single cohort of $CD45.2^+$ thymocytes from a thymus lacking CCL21Ser into WT peripheral tissues where CCR7L were expressed normally. Comparable thymocyte cellularities in $Ccl21a^{-/-}$ and $Ccl21a^{+/-}$ thymuses before and after transplantation indicated no gross changes in T-cell development (Figure 3B; supplemental Figure 3). Importantly however, after transplantation, we saw significantly fewer cSP4 and SP8 RTEs in spleens of WT mice receiving $Ccl21a^{-/-}$ thymic lobes (Figure 3C-D). Thus, absence of intrathymic CCL21Ser leads to reduced RTEs in WT peripheral tissues, which argues in favor of an important role for this chemokine in neonatal thymus emigration.

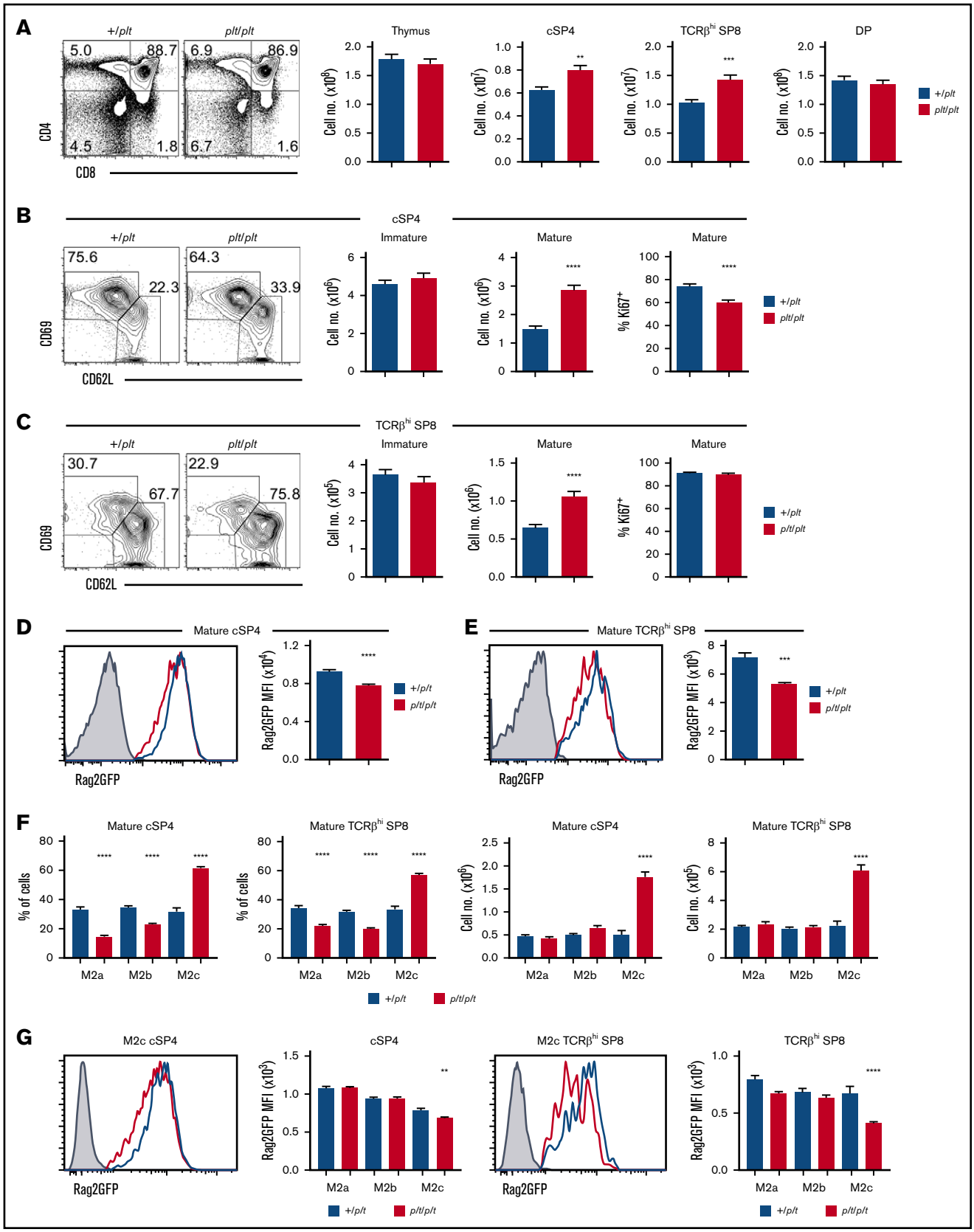

Figure 1. CCR7L deficiency prolongs the intrathymic dwell time Of neonatal SP thymocytes. (A-C) Flow cytometric analysis of thymocytes in *plt/plt* (n = 16) and *+/plt* (n = 16) littermate postnatal day–10 neonatal mice. cSP4 were gated as $CD4^{+}TCR\beta^{hi}CD25^{-}Foxp3^{-}$, SP8 as $CD8^{+}TCR\beta^{hi}$, immature SP as $CD69^{+}CD62L^{-}$, and mature

Neonatal thymic expression of *Ccl21a* selectively maps to mTEC subsets

Given the importance of CCL21Ser in regulating neonatal thymus emigration, we next analyzed patterns of *Ccl21a* gene expression in cellular compartments of the neonatal thymus. Here, we used *Ccl21a*^{tdTom} reporter mice,[27] and background levels of tdTomato were set using WT controls. Thymic lobes were enzymatically digested and subdivided into CD45$^-$EpCAM1$^+$ TECs and CD45$^+$ hemopoietic cells. In agreement with expression patterns reported for adult thymus,[27] *Ccl21a* was detectable in EpCAM1$^+$ TECs but not hemopoietic cells (Figure 4A). Further analysis of non-TEC stromal compartments showed *Ccl21a* expression was undetectable in CD45$^-$EpCAM1$^-$CD31$^+$ endothelium and CD45$^-$EpCAM1$^-$CD31$^-$ mesenchyme, indicating *Ccl21a* is selectively expressed by TECs in neonatal thymus (Figure 4A). By subdividing TECs into cortical TECs and mTECs, we found EpCAM1$^+$Ly51$^+$UEA1$^-$ cTECs lacked *Ccl21a* expression, whereas EpCAM1$^+$Ly51$^-$UEA1$^+$ mTECs expressed *CCL21a*^{tdTom} at varying levels (Figure 4B). Interestingly, further subdivision of bulk mTECs using MHC II and CD80 expression revealed ~50% of both MHCII^{hi}CD80^{hi} mTECs^{hi} and MHCII^{lo}CD80^{lo} mTECs^{lo} were *Ccl21a*$^{tdTom+}$ (Figure 4C). Thus, *Ccl21a* is expressed by multiple mTEC subsets in the neonatal thymus. Importantly, and in line with flow cytometry, confocal microscopy of *Ccl21a*^{tdTom} of thymus sections from *Ccl21a* heterozygous mice demonstrated restricted expression to thymus medulla (Figure 4D). Thus, analysis of the cellular distribution and anatomic location of *Ccl21a* expression by stromal microenvironments in neonatal thymus indicates its selective expression by mTECs.

CCL21 protein presentation at sites of thymic exit

Because exit of mature SP thymocytes from thymus involves migration toward blood vessels at the CMJ,[16,18] we wondered how mTECs restricted gene expression of *Ccl21a* related to its importance in neonatal thymic exit. To identify and compare sites of chemokine production and localization, we performed confocal microscopy of WT neonatal thymus sections using anti-CCL21 antibody to analyze distribution of CCL21 protein within medullary environments. Sections were costained with ERTR5 and anti-CD31 to detect mTECs and blood vessels, respectively. CCL21 protein was detected in medullary areas, including in ERTR5$^+$ mTECs (Figure 5A). Staining observed with anti-CCL21 antibody was specific; no signal was observed when the same reagent was used on *Ccl21a*$^{-/-}$ thymus sections (Figure 5B). Interestingly, closer investigation revealed CCL21 protein was associated with ERTR5$^+$ mTECs and CD31$^+$ blood vessels at the CMJ, but not with cortical CD31$^+$ vessels (Figure 5A,C). Indeed, higher magnification of CCL21$^+$ vessels at the CMJ indicated CCL21 protein accumulated around CD31$^+$ endothelial cells (Figure 5C). Collectively, these findings demonstrate the mTEC product CCL21 does not show even distribution in the thymus medulla. Rather, this chemokine is concentrated at CMJ blood vessels representing sites of thymic exit.

Thymic blood vessels are surrounded by concentric layers of mesenchyme (Figure 5D), where an outer layer of adventitial cells surrounds pericytes that ensheath CD31$^+$ endothelial cells.[17,18,35] Given the close proximity of both mesenchymal cell types to sites of CCL21 accumulation, we examined their relationship with CCL21 protein distribution. Using flow cytometric analysis of digested WT neonatal thymus, we identified pericytes as CD45$^-$EpCAM1$^-$CD31$^-$CD34$^-$integrin $\alpha7^+$ cells[35] and adventitial mesenchymal cells as CD45$^-$EpCAM1$^+$CD31$^-$CD34$^+$integrin $\alpha7^-$ cells[35] (Figure 5D). To investigate their possible involvement in CCL21 localization, we examined the ability of thymic stromal subsets within digested *plt*/*plt* thymus to immobilize and present RFP-tagged recombinant CCL21. Thymus suspensions were incubated with full-length CCL21-mRFP protein and then stained with antibodies identifying stromal subsets. Interestingly, pericytes and adventitial cells clearly bound CCL21-mRFP protein, with a small but significant increase in adventitial cells compared with pericytes (Figure 5E). In contrast, little or no CCL21-mRFP binding by TECs or endothelium was observed (Figure 5E), with RFP fluorescence levels comparable to those of controls. Thus, the ability to capture and present CCL21 is restricted to specific thymic stromal subsets, namely pericytes and adventitial cells.

For T-cell migration in peripheral tissues, CCL21 is captured and immobilized by blood vessel–associated extracellular matrix (ECM) components.[36,37] To facilitate this, CCL21 contains a positively charged C-terminal domain that binds to negatively charged ECM components, including heparin-like glycosaminoglycans (GAGs).[9,38] We therefore examined whether CCL21-mRFP binding by thymic pericytes and adventitial mesenchyme might operate similarly. We incubated neonatal *plt*/*plt* thymus suspensions with full-length CCL21-mRFP or tCCL21-mRFP, which lacked the charged C-terminal extension, and assessed binding to thymic stromal populations by flow cytometry. Importantly, and in contrast to full-length CCL21-mRFP, neither pericytes nor adventitial cells bound tCCL21-mRFP (Figure 5F), indicating the C-terminal region of CCL21 is essential for immobilization by thymic stroma. Moreover, and in line with this, both pericytes and adventitial cells showed minimal binding of an RFP-conjugated form of CCL19, a CCR7L that lacks the C-terminal domain contained within CCL21 (Figure 5F). Thus, mesenchymal stromal cells surrounding sites of thymic exit capture and present mTEC-derived CCL21 at their surface, and this requires the C-terminal extension of CCL21 capable of ECM binding.

Figure 1. (continued) SP as CD69$^-$CD62L$^+$. Percentages of cSP4 and SP8 expressing Ki67 are also shown in panels B and C. (E-D) Rag2GFP levels in cSP4 and SP8 thymocytes from Rag2GFP*plt*/*plt* mice (n = 5; red) and Rag2GFP+/*plt* controls (n = 7; blue). Gray histograms indicate nonfluorescent control cells. (F) Numbers and frequencies of M2a, M2b, and M2c subsets of mature CD69$^-$CD62L$^+$ cSP4 and SP8 in Rag2GFP+/*plt* (n = 16) controls and Rag2GFP *plt*/*plt* mice (n = 16). Bar chart indicates percentages of each subset in Rag2GFP+/*plt* (blue bars) and Rag2GFP *plt*/*plt* (red bars). (G) Rag2GFP levels in the M2c subset of cSP4 and SP8 thymocytes from +/*plt* controls (n = 7; blue) and plt/plt (n = 5; red) mice. Bar charts show percentages of M2a, M2b, and M2c subsets of cSP4 and SP8 in +/*plt* (blue bars) and *plt*/*plt* (red bars). For analysis of data in panels F and G, multiple comparison analysis was achieved by a 2-way analysis of variance followed by Sidak's posttest in GraphPad Prism to determine statistical differences. In all cases, error bars represent mean ± SEM. Flow cytometric data representative of at least 3 independent experiments. $^{**}P < .01$, $^{***}P < .001$, $^{****}P < .0001$. DP, double positive; MFI, mean fluorescence intensity.

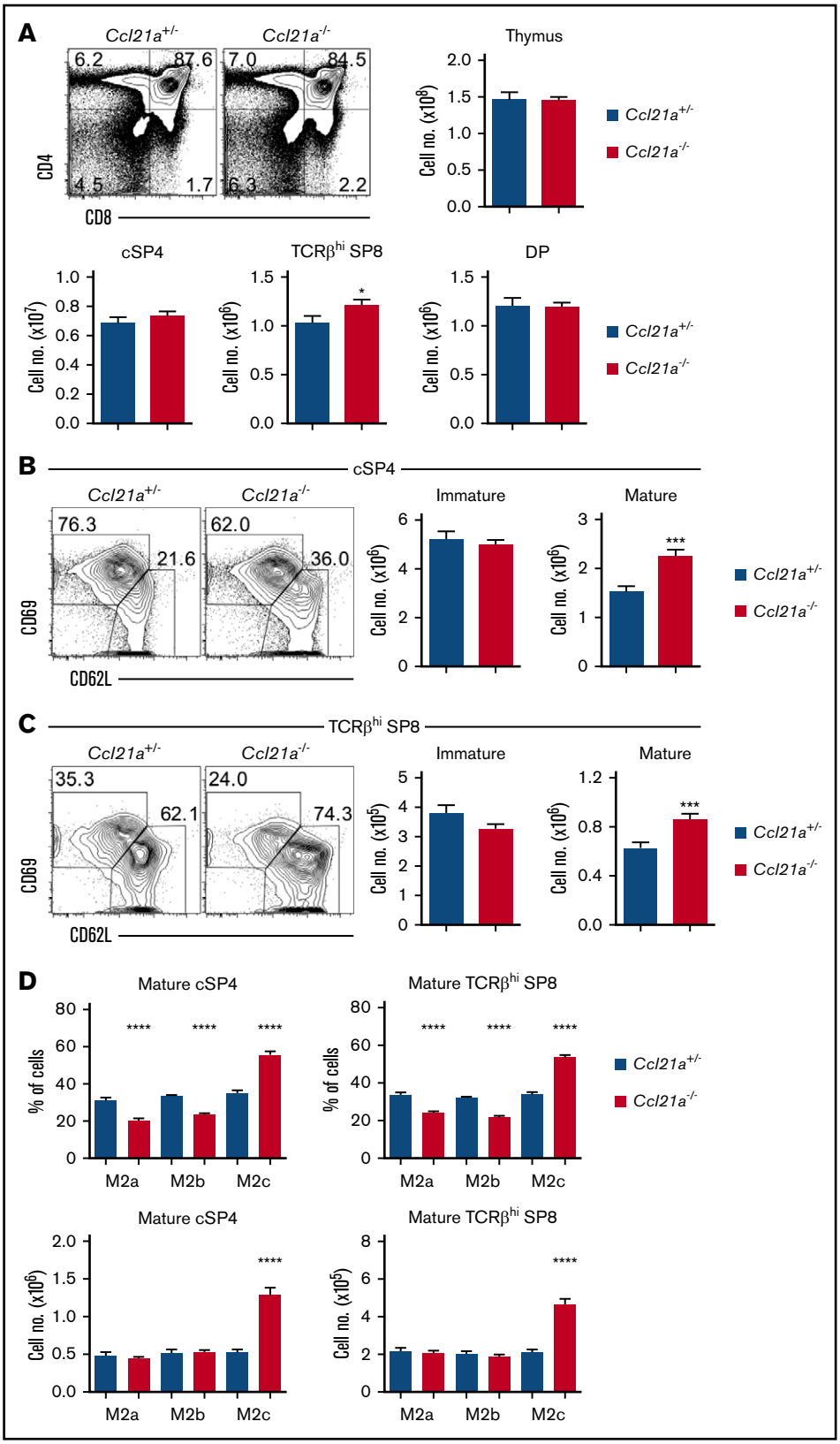

Figure 2. CCL21 is important for neonatal SP thymocyte egress. (A) Flow cytometric analysis and quantitation of CD4/CD8 thymocyte subsets from postnatal day−10 (P10) *Ccl21a*$^{-/-}$ (n = 15; red bars) and *Ccl21a*$^{+/-}$ (n = 16; blue bars) littermate controls. Quantitation of immature CD69^{+} CD62L^{-} and mature CD69^{-}CD62L^{+} subsets of cSP4 (B) and TCRβ^{hi} SP8 (C) thymocytes in *Ccl21a*$^{-/-}$ (n = 15; red bars) and *Ccl21*$^{+/-}$ (n = 16; blue bars) littermate P10 neonatal mice. (D) Numbers and frequencies of M2a, M2b, and M2c subsets of cSP4 and SP8 thymocytes in *Ccl21a*$^{+/-}$ (blue bars) and *Ccl21a*$^{-/-}$ (red bars) mice. For analysis of data in panel D, multiple comparison analysis was achieved by a 2-way analysis of variance followed by Sidak's posttest in GraphPad Prism to determine statistical differences. In all cases, error bars represent mean ± SEM. Flow cytometric data representative of 3 independent experiments. *$P < .05$, ***$P < .001$, ****$P < .0001$.

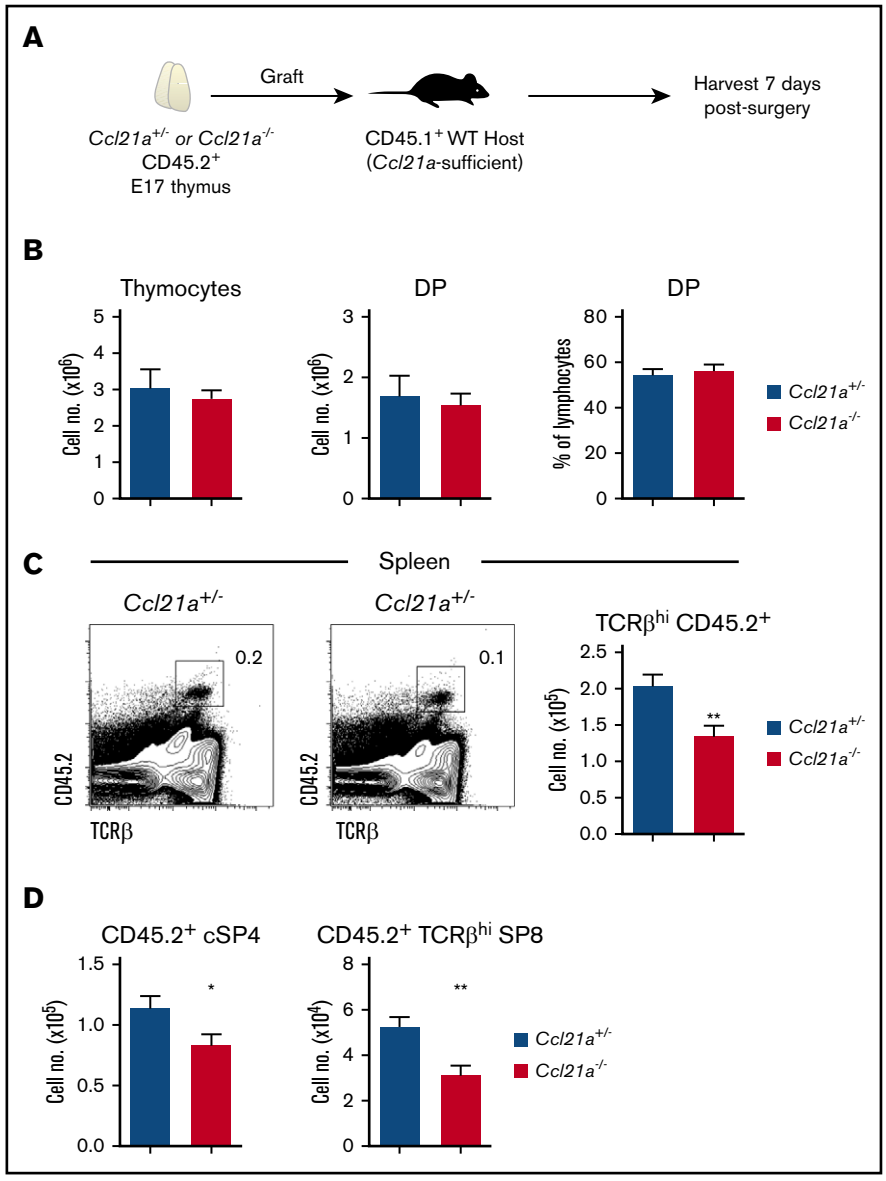

Figure 3. Thymus-specific CCL21 deficiency decreases RTE frequency in WT peripheral tissues. (A) Schematic of the experimental approach used to measure thymic output from *Ccl21a*-deficient thymus. Freshly isolated E17 CD45.2$^+$ *Ccl21a*$^{+/-}$ or *Ccl21a*$^{-/-}$ thymic lobes were grafted under the kidney capsule of CD45.1$^+$ WT hosts. Spleens were harvested from host mice 7 days after surgery. (B) Quantitation of total thymocyte numbers, and the number and proportion of CD4$^+$CD8$^+$ double-positive (DP) thymocytes in E17 *Ccl21a*$^{+/-}$ (n = 10) or *Ccl21a*$^{-/-}$ (n = 11) thymic lobes before transplantation. Flow cytometric detection and quantitation of donor thymus–derived CD45.2$^+$TCRβ^{hi} T cells (C) and CD45.2$^+$TCRβ^{hi} cSP4 and CD45.2$^+$TCRβ^{hi} SP8 T cells (D) in the spleens of WT mice that received either *Ccl21a*$^{+/-}$ (n = 8; blue bars) or *Ccl21a*$^{-/-}$ (n = 8; red bars) grafts. Error bars represent mean ± SEM. Flow cytometric data representative of at least 3 independent experiments. *$P < .05$, **$P < .01$.

Thymic mesenchyme presents CCL21 via heparan sulfate

In lymph nodes, heparan sulfate is a GAG that captures CCL21 for T-cell migration.[36] Given the presentation of CCL21 by thymic mesenchyme, we next analyzed intrathymic expression of heparan sulfate via flow cytometry. Hemopoietic and endothelial cells lacked detectable heparan sulfate expression, with only a small shift in fluorescence detectable in TECs (Figure 6A-B). In contrast, pericytes and adventitial cells showed high levels of heparan sulfate expression (Figure 6A), with the highest levels detectable on adventitial cells (Figure 6B). Consistent with this selective expression, heparan sulfate was also detectable around CD31$^+$ thymic blood vessels in thymus sections that represent sites of adventitial mesenchyme, pericytes and CCL21 protein accumulation (Figure 6C).

To examine the functional importance of heparan sulfate in mesenchymal presentation of CCL21, thymus sections were treated with heparinase III, an enzyme that digests heparan sulfate,[39,40] and then stained with antibodies specific for either intact heparan sulfate or its digested form (Δ-heparan sulfate).[36] Untreated thymus sections showed positive staining for heparan sulfate around CD31$^+$ blood vessels (Figure 7A upper panels), and the digested form of Δ-heparan sulfate was barely detectable (Figure 7A lower panels). In contrast, treatment with heparinase III before antibody staining abrogated detection of heparan sulfate (Figure 7B upper panels) and resulted in the detection of Δ-heparan sulfate (Figure 7B lower panels). Consistent with this, flow cytometric analysis showed that pericytes and adventitial mesenchyme stained positively for heparan sulfate but not Δ-heparan sulfate before heparinase III treatment (Figure 7C), whereas the converse was apparent after enzyme treatment (Figure 7D). Significantly, pretreatment of thymic stromal suspensions with heparinase III before incubation with CCL21-mRFP significantly reduced chemokine presentation by both adventitial mesenchyme and pericytes (Figure 7E). Together, these findings indicate adventitial mesenchyme and pericytes represent distinct

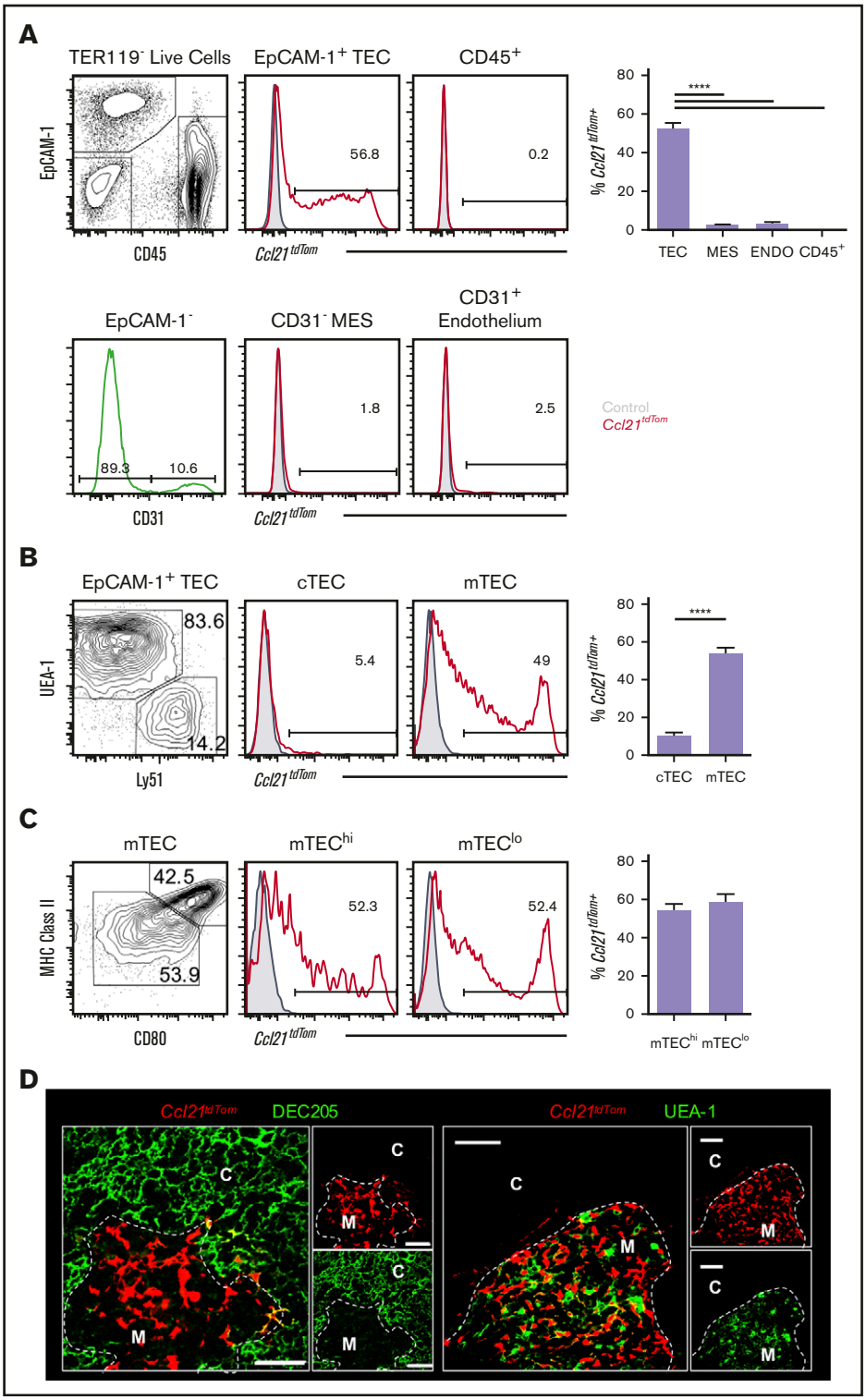

Figure 4. *Ccl21a* gene expression in the neonatal thymus is restricted to mTECs. (A) Flow cytometric analysis and quantitation of tdTomato expression in total CD45$^+$ thymocytes and the indicated thymic stromal populations in postnatal day–10 (P10) heterozygous *Ccl21a*^{tdTom} mice (n = 8). Thymic mesenchyme was identified as CD45$^-$CD31$^-$EpCAM1$^-$ cells. Red lines indicate tdTomato staining levels in heterozygous *Ccl21a*^{tdTom} mice; gray histograms indicate nonfluorescent control cells. Flow cytometric plots and analysis representative of 3 independent experiments. (B) Analysis of *Ccl21a*^{tdTom} expression in P10 EpCAM1$^+$Ly51$^+$UEA1$^-$ cTECs and EpCAM1$^+$Ly51$^-$UEA1$^+$ mTECs. (C) *Ccl21a*^{tdTom} expression after subdivision of total mTECs into MHCII^{low}CD80^{low} (mTEC^{lo}) and MHCII^{hi}CD80^{hi} (mTEC^{hi}) subsets (n = 10). In all cases, error bars represent mean ± SEM. For analysis of data in panel A, multiple comparison analysis was achieved by a 1-way analysis of variance followed by Tukey's posttest in GraphPad Prism to determine statistical differences. In panel D, confocal microscopy was used to show tdTomato expression in heterozygous *Ccl21a*^{tdTom} P10 mice alongside identification of cTECs with either anti-CD205 (green) or mTECs with UEA1 (green); dotted line denotes the CMJ. Scale bars represent 50 μm. Images shown are representative of 3 mice. ****$P < .0001$. C, cortex; M, medulla; MHC, major histocompatibility complex.

stromal compartments that present mTEC-derived CCL21 at sites of thymic exit, which involves heparan sulfate–mediated immobilization and presentation of CCL21.

Discussion

In murine neonates, thymus emigration of conventional αβT cells is critical to establish T-cell compartments for protective immunity. This process is also necessary to avoid autoimmunity caused by disruption of the ordered emigration of conventional and then regulatory T cells that occurs in the neonate.[10-12] Here, we show absence of CCR7L promotes accumulation of mature CD62L$^+$ SP thymocytes and prolongs their intrathymic dwell time. Comparison of *Ccl19*$^{-/-}$ and *Ccl21a*$^{-/-}$ mice indicated defects occur as a result of a requirement for CCL21Ser but not CCL19. Because both

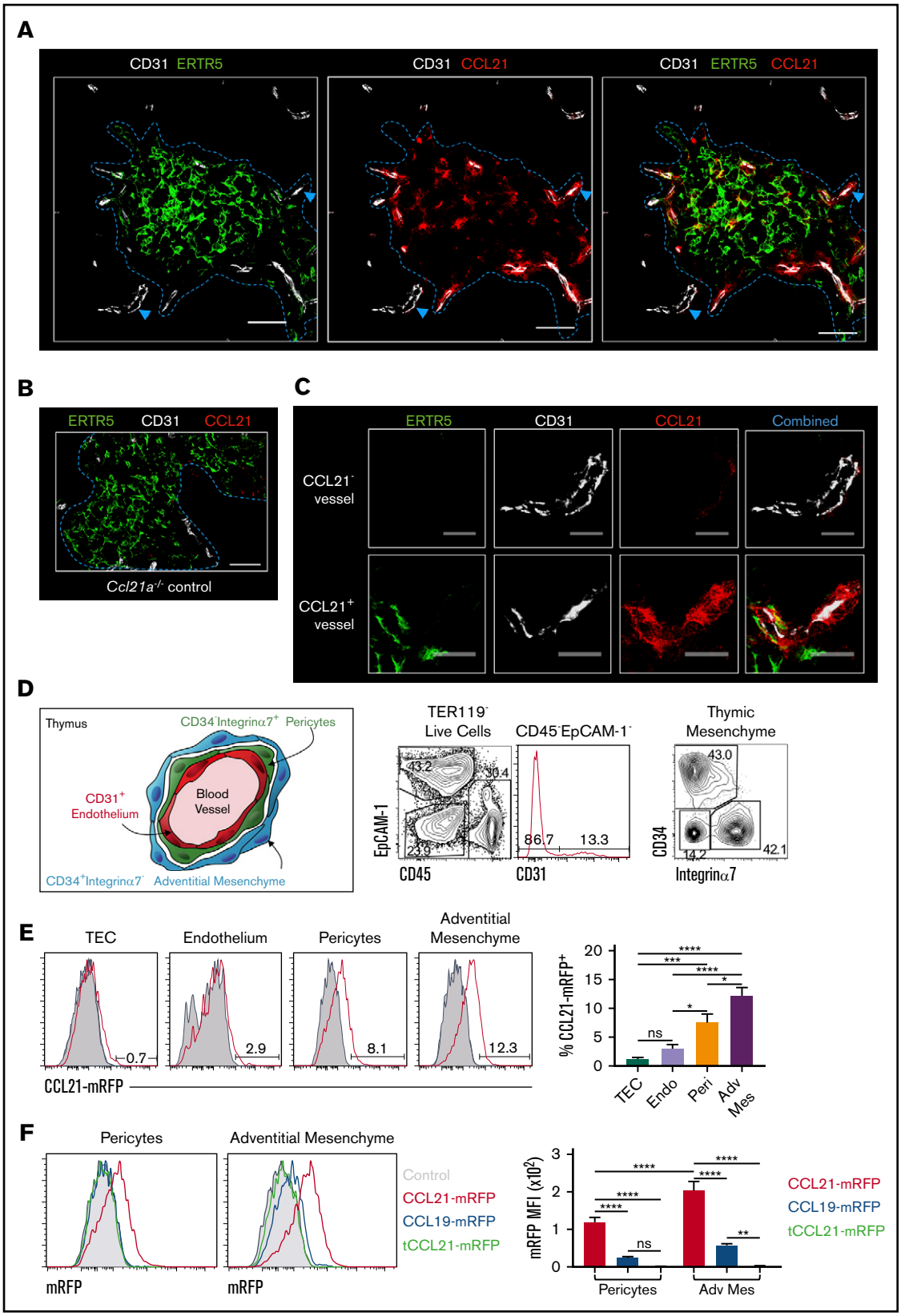

Figure 5. CCL21 protein is presented by thymic mesenchyme at sites of thymic exit. (A) Confocal images of thymus sections from postnatal day–10 (P10) WT mice stained with antibodies to the endothelial marker CD31 (white), mTEC marker ERTR5 (green), and CCL21 protein (red). Blue dotted line indicates the CMJ, and blue arrows indicate vessels investigated at higher magnification in panel C. (B) Image of a thymus section from a *Ccl21a* knockout P10 mouse stained with anti-CCL21 (red), anti-CD31

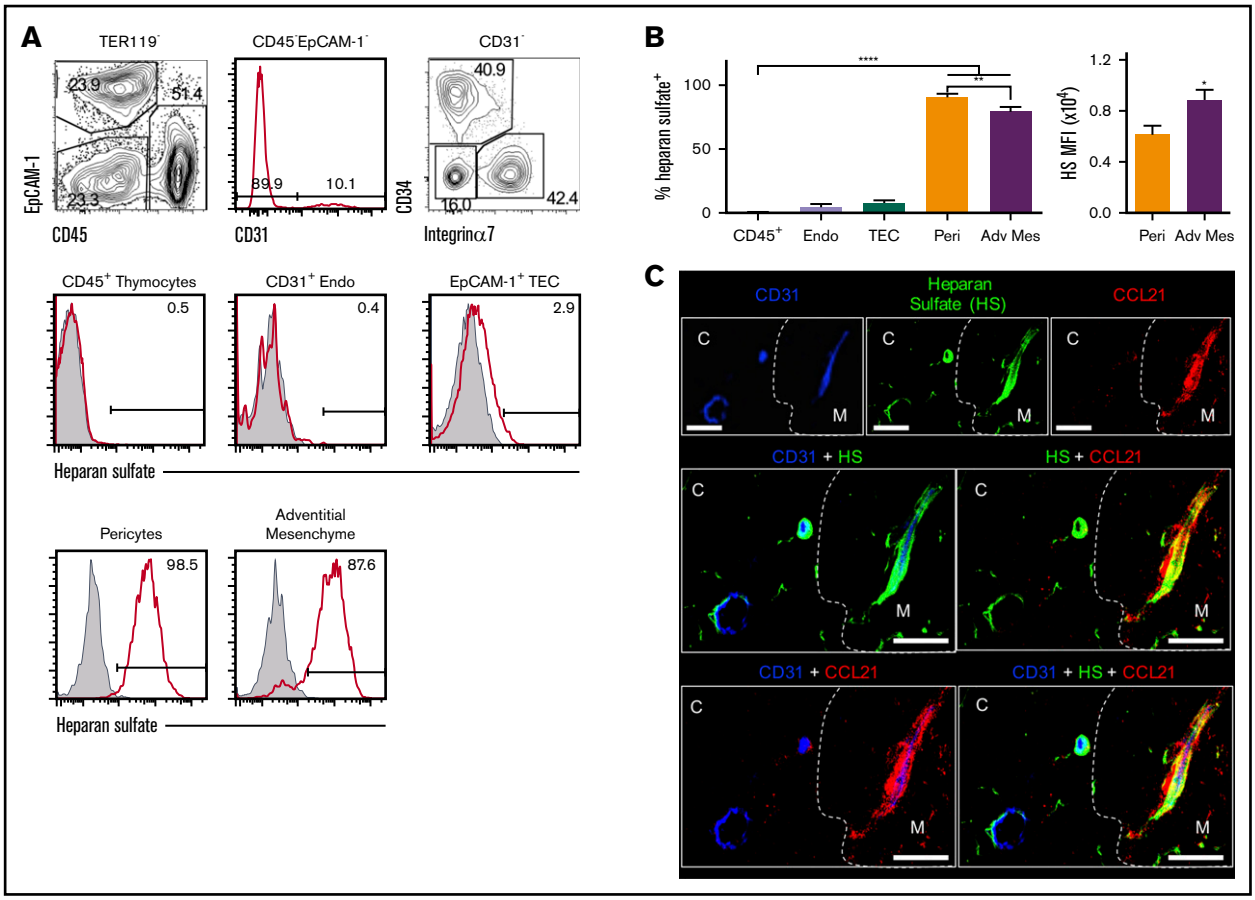

Figure 6. Thymic heparan sulfate is restricted to adventitial mesenchyme and pericytes. Flow cytometric analysis (A) and quantitation (B) of heparan sulfate expression by CD45$^+$ thymocytes, CD31$^+$ endothelium, EpCAM-1$^+$ TECs, CD34$^-$integrin $\alpha7^+$ pericytes, and CD34$^+$integrin $\alpha7^-$ adventitial mesenchyme in postnatal day–10 (P10) WT thymus. Gray filled histograms indicate staining levels where no anti–heparan sulfate primary antibody was added. (B) Analysis of mean fluorescence intensity (MFI) of heparan sulfate (HS) on CD34$^-$integrin $\alpha7^+$ pericytes (orange bar) and CD34$^+$integrin $\alpha7^-$ adventitial mesenchyme (purple bar) after gating on HS-expressing cells. Data shown from 3 separate experiments with a total of mice. Error bars in panel B represent mean ± SEM. For analysis of data in panel B, multiple comparison analysis was achieved by a 1-way analysis of variance followed by Tukey's posttest in GraphPad Prism to determine statistical differences. (C) Confocal images of thymus sections from a P10 WT mouse stained with anti-CD31 (blue), anti-HS (green), and anti-CCL21 protein (red). White dotted line indicates the CMJ. Scale bar denotes 20 μm. Images shown representative of 5 mice. *$P < .05$, ** $P < .01$, ****$P < .0001$. C, cortex; M, medulla.

CCL19 and CCL21Ser are expressed by thymic stroma,[9,41,42] the requirement for CCL21Ser cannot be explained by lack of CCL19 availability. Rather, CCL21Ser seems specialized in controlling neonatal thymus emigration, a finding that is important in relation to previous work implicating CCL19 in this process.[9] For example, earlier studies showed recombinant CCL19, but not CCL21, induced SP thymocyte egress from fetal thymus organ cultures. Furthermore, treatment of WT neonates with neutralizing anti-CCL19

Figure 5. (continued) (white), and ERTR5 (green). Note the absence of CCL21 staining. Scale bars in panels A and B denote 50 μm. (C) High-power images of CCL21$^-$ (upper panels) and CCL21$^+$ (lower panels) vessels identified by blue arrowheads in panel A. Images show individual channels for ERTR5 (green), CD31 (white), and CCL21 protein (red), as well as a combined image showing all markers simultaneously. Scale bars denote 25 μm. Data are representative of 4 mice from 2 separate experiments. (D) Schematic diagram and flow cytometric analysis of thymic mesenchymal populations associated with thymic blood vessels. Schematic is based on findings of Sitnik et al[35] and demonstrates CD34$^-$integrin $\alpha7^+$ pericytes and CD34$^+$integrin $\alpha7^-$ adventitial mesenchymal cells that surround thymic blood vessels. Flow cytometric analysis shows identification of these populations in P10 WT thymus. (E) Flow cytometric analysis of presentation of CCL21-mRFP by indicated thymic stromal populations in *plt/plt* P10 thymus suspensions. Gray histograms represent control staining seen in the absence of CCL21-mRFP. Bar chart indicates percentages of CCL21-mRFP$^+$ cells within each stromal subset. (F) Flow cytometric analysis of stromal cell presentation of full-length CCL21-mRFP (red), full-length CCL19-mRFP (blue), or tCCL21-mRFP (green) by CD34$^-$ integrin $\alpha7^+$ pericytes and CD34$^+$integrin $\alpha7^-$ adventitial mesenchymal cells. Gray filled histograms represent staining levels observed when no chemokines were added. Bar chart shows mRFP mean fluorescence intensity (MFI) for each fluorescent chemokine and indicated stromal cell type. For analysis of data in panels E and F, multiple comparison analysis was achieved by a 1-way analysis of variance (ANOVA) followed by Tukey's post-test (E) or 2-way ANOVA followed by Sidak's posttest (F) in GraphPad Prism to determine statistical differences. All data shown representative of 3 independent experiments, with a total of 7 to 11 mice for each analysis. Error bars represent mean ± SEM. *$P < .05$, **$P < .01$, ***$P < .001$, ****$P < .0001$.

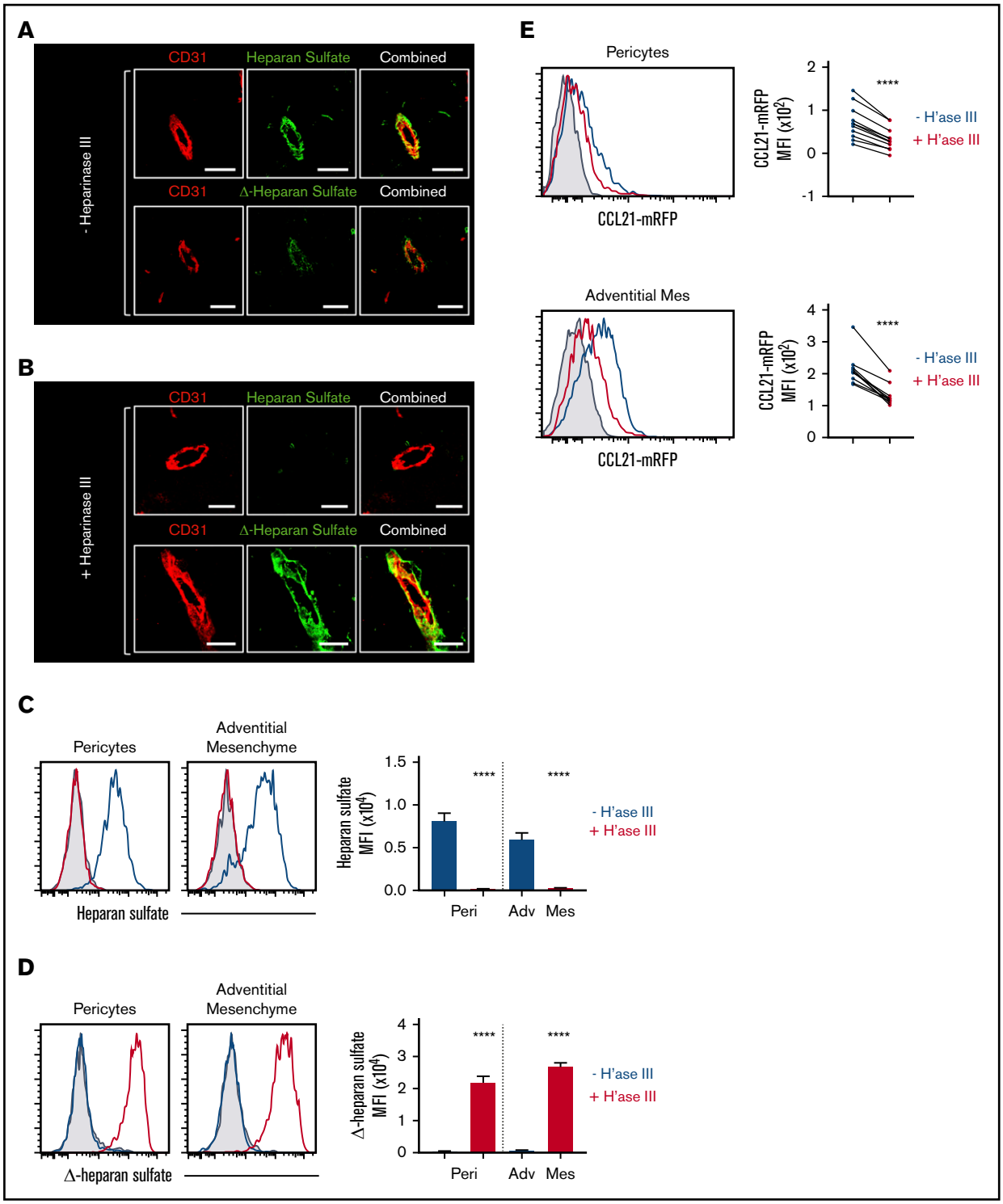

Figure 7. Heparan sulfate mediates CCL21 presentation at sites of thymic exit. (A) Confocal image of a blood vessel in a WT postnatal day–10 (P10) thymus section stained with anti-CD31 (red) and either anti–heparan sulfate (green; upper images) or an antibody to detect Δ-heparan sulfate (green; lower images). (B) Confocal images as in panel A, but sections were treated with heparinase III (H'ase III) enzyme before antibody staining. Scale bars denote 20 μm. Images typical of 2 separate experiments involving at least 3 mice. (C) Flow cytometric analysis of heparan sulfate expression by pericytes and adventitial mesenchyme before (blue histogram and blue bar) and after (red histogram and red bar) heparinase III treatment. (D) Flow cytometric analysis of Δ-heparan sulfate expression by pericytes and adventitial mesenchyme before (blue histogram and blue bar) or after (red histogram and red bar) heparinase III treatment. Bar charts in panels C and D show mean fluorescence intensity (MFI) expression levels of heparan sulfate and Δ-heparan sulfate, respectively. Data from 3 experiments with a minimum of 8 mice. (E) Flow cytometric analysis of CCL21m-RFP chemokine presentation by adventitial mesenchyme (upper panels) and pericytes (lower panels) in digested P10 WT thymus samples before (blue line) and after (red line) heparinase III treatment. Gray histograms represent control staining where no chemokine was added. Data from 3 separate experiments and 11 mice. Error bars represent mean ± SEM. Paired Student *t* tests were performed for statistical analysis of data in panel E. ****$P < .0001$.

antibodies reduced αβT cells in the spleen.[9] The explanation for the discrepancy in these findings and those presented here is unclear. One possibility is differences in the experimental systems used. Whereas Ueno et al[9] used both in vivo and in vitro approaches (fetal thymus organ cultures), we used in vivo and ex vivo approaches throughout our study. Thus, the requirements for in vitro thymus emigration may differ to those in vivo. Additionally, becAUSE CCL19 controls αβT-cell entry into the spleen,[34] decreased splenic T-cell numbers after anti-CCL19 treatment may be due to inhibition of CCL19 in peripheral tissues. Alternatively, anti-CCL19 treatment may alter peripheral lymphoid tissues, which then alters thymus emigration in a thymus-extrinsic manner. Interestingly, analysis of peripheral T-cell numbers in CCL21-deficient mice showed a reduction of these cells in lymph nodes (data not shown), which again may be due to the reasons outlined above. In sum, we agree with Ueno et al[9] on an important role for CCR7 in neonatal thymus emigration. Regarding current data on the roles of individual ligands, our data point toward an intrathymic requirement for CCL21 but not CCL19 in this process. However, a role for CCL19 in peripheral tissues is not ruled out, which would perhaps go some way toward explaining differences between our study and that by Ueno et al.[9]

As in adults,[27] we found *Ccl21a* expression in neonates mapped to mTECs. Importantly, CCL21 protein accumulated at blood vessels representing sites of emigration, which involved heparan sulfate–mediated presentation by pericytes and adventitial mesenchyme. Interestingly, although enzyme treatment of thymic stroma completely abolished heparan sulfate expression by adventitial cells and pericytes, we still saw low-level CCL21 binding by these cells. One possible explanation for this is that other GAGs produced by these cell types can also contribute to CCL21 capture by thymic stroma. Whatever the case, because CCL21 production is limited to mTECs, whereas CCL21 presentation is a function of pericytes and adventitial cells, this dichotomy underlines the requirement for thymic stromal heterogeneity and identifies functional synergy between TECs and mesenchyme. Interestingly, although we identified roles for both pericytes and adventitial cells within thymic mesenchyme, it is not known whether additional subdivisions occur within these cell types that may relate to their capacity to capture chemokines such as CCL21. Additional studies are required to gain a better understanding of thymic mesenchyme heterogeneity and how it may relate to possible functional specialization. Importantly, CCL21 immobilization and presentation required the positively charged C-terminal extension that allows binding to negatively charged ECM components. Because CCL19 lacks this domain, this fits with its failure to be captured by stroma and mirrors lymph node entry of peripheral T cells, which involves heparan sulfate–mediated CCL21.[36] Of note, it is unclear how disruption of intrathymic CCR7-CCL21 interactions results in impaired emigration. One possibility is that this occurs because of the disrupted medullary organization in neonatal *Ccl21a*$^{-/-}$ mice (data not shown), which has also been reported in adult *Ccl21a*$^{-/-}$ mice.[27] Alternatively, defective emigration may map to the requirement for CCL21 in controlling dendritic cells,[43] which have been linked to control of thymus emigration.[44] Further work is needed to examine these possibilities.

The requirement for CCL21 in thymus emigration extends our understanding of this chemokine in thymus biology, which includes control of cortex-medulla migration in the adult.[27] Related to this, although CCR7 plays additional roles in thymocyte development, including progenitor entry to thymus,[45-47] CD4^{-}CD8^{-} precursor positioning,[48] and control of the Foxp3^{+} regulatory T-cell pool,[2,49] it is unclear if these requirements require CCL21 or CCL19. Also, unlike in the neonate, adult thymic egress is CCR7 independent.[19] It is not known why CCR7 and CCR7L regulate neonatal thymus emigration but are dispensable in adults. One possibility is that in the absence of CCR7-mediated migration, adult SP thymocytes exit via blood vessels present in other thymic sites, and such alternate sites may not be available in neonatal thymus. Another possibility is neonatal T-lymphopenia provides feedback that influences thymus emigration. Whatever the explanation, these findings emphasize age-related differences in control of thymus emigration. Of note, it will be interesting to examine whether thymus emigration of γδT cells, including invariant γδT cells in embryonic periods,[50,51] depends upon CCR7/CCL21.

In sum, by examining mechanisms controlling αβT-cell emigration from neonatal thymus, we identify CCL21Ser as an important regulator. These findings extend our understanding of an essential step in immune system formation, as well as the known functions of CCL21 in thymus biology. The collective control of chemokine production and distribution by thymic epithelium and mesenchyme emphasizes the functional importance of stromal cell heterogeneity in T-cell development.

Acknowledgments

The authors thank Sanjiv Luther for providing *Ccl19*$^{-/-}$ mice, all laboratory members for their critical reading of the manuscript, and Andi Bacon and Biomedical Services Unit staff for animal husbandry. The authors also thank Douglas Dyer for helpful discussions.

This work was supported by Medical Research Council program grant MR/N000919/1 (G.A.); Swiss National Science Foundation grant 310030 189144 (D.F.L.); Japan Society for the Promotion of Science grant 17K08884 and NOVARTIS Foundation (Japan) for the Promotion of Science grant 274-1283 (I.O.); and the Intramural Research Program of the US National Institutes of Health, the National Cancer Institute, and the Center for Cancer Research (Y.T.).

Authorship

Contribution: K.D.J. designed and performed experiments, analyzed data, performed statistical analysis, and wrote the manuscript; A.J.W. designed and performed experiments; D.F.L., V.P., I.O., Y.T., and S.M.P. provided key reagents and expert advice in experimental design and methodology; and G.A. and W.E.J. designed experiments, analyzed data, and wrote the manuscript.

Conflict-of-interest disclosure: The authors declare no competing financial interests.

ORCID profiles: K.D.J., 0000-0001-8811-6996; D.F.L., 0000-0001-8610-4764; Y.T., 0000-0002-4992-9174; W.E.J., 0000-0003-3422-8372; G.A., 0000-0002-2917-4085.

Correspondence: Graham Anderson, Institute for Immunology and Immunotherapy, Floor 4 Institute for Biomedical Research, Medical School, University of Birmingham, Birmingham B15 2TT, United Kingdom; e-mail: g.anderson@bham.ac.uk.

References

1. Webb LV, Ley SC, Seddon B. TNF activation of NF-κB is essential for development of single-positive thymocytes. *J Exp Med*. 2016;213(8):1399-1407.
2. Hsu FC, Shapiro MJ, Chen MW, et al. Immature recent thymic emigrants are eliminated by complement. *J Immunol*. 2014;193(12):6005-6015.
3. Xing Y, Wang X, Jameson SC, Hogquist KA. Late stages of T cell maturation in the thymus involve NF-κB and tonic type I interferon signaling. *Nat Immunol*. 2016;17(5):565-573.
4. Boehm T, Scheu S, Pfeffer K, Bleul CC. Thymic medullary epithelial cell differentiation, thymocyte emigration, and the control of autoimmunity require lympho-epithelial cross talk via LTbetaR. *J Exp Med*. 2003;198(5):757-769.
5. James KD, Jenkinson WE, Anderson G. T-cell egress from the thymus: should I stay or should I go? *J Leukoc Biol*. 2018;104(2):275-284.
6. Gabor MJ, Godfrey DI, Scollay R. Recent thymic emigrants are distinct from most medullary thymocytes. *Eur J Immunol*. 1997;27(8):2010-2015.
7. Drennan MB, Elewaut D, Hogquist KA. Thymic emigration: sphingosine-1-phosphate receptor-1-dependent models and beyond. *Eur J Immunol*. 2009; 39(4):925-930.
8. Kelly KA, Scollay R. Seeding of neonatal lymph nodes by T cells and identification of a novel population of CD3-CD4+ cells. *Eur J Immunol*. 1992;22(2): 329-334.
9. Ueno T, Hara K, Willis MS, et al. Role for CCR7 ligands in the emigration of newly generated T lymphocytes from the neonatal thymus. *Immunity*. 2002; 16(2):205-218.
10. Asano M, Toda M, Sakaguchi N, Sakaguchi S. Autoimmune disease as a consequence of developmental abnormality of a T cell subpopulation. *J Exp Med*. 1996;184(2):387-396.
11. Nishizuka Y, Sakakura T. Thymus and reproduction: sex-linked dysgenesia of the gonad after neonatal thymectomy in mice. *Science*. 1969;166(3906):753-755.
12. Taguchi O, Nishizuka Y, Sakakura T, Kojima A. Autoimmune oophoritis in thymectomized mice: detection of circulating antibodies against oocytes. *Clin Exp Immunol*. 1980;40(3):540-553.
13. McCaughtry TM, Wilken MS, Hogquist KA. Thymic emigration revisited. *J Exp Med*. 2007;204(11):2513-2520.
14. James KD, Cosway EJ, Lucas B, et al. Endothelial cells act as gatekeepers for LTβR-dependent thymocyte emigration. *J Exp Med*. 2018;215(12): 2984-2993.
15. Scollay R, Godfrey DI. Thymic emigration: conveyor belts or lucky dips? *Immunol Today*. 1995;16(6):268-273, NaN-274.
16. Mori K, Itoi M, Tsukamoto N, Kubo H, Amagai T. The perivascular space as a path of hematopoietic progenitor cells and mature T cells between the blood circulation and the thymic parenchyma. *Int Immunol*. 2007;19(6):745-753.
17. Matloubian M, Lo CG, Cinamon G, et al. Lymphocyte egress from thymus and peripheral lymphoid organs is dependent on S1P receptor 1. *Nature*. 2004; 427(6972):355-360.
18. Zachariah MA, Cyster JG. Neural crest-derived pericytes promote egress of mature thymocytes at the corticomedullary junction. *Science*. 2010; 328(5982):1129-1135.
19. Ueno T, Saito F, Gray DH, et al. CCR7 signals are essential for cortex-medulla migration of developing thymocytes. *J Exp Med*. 2004;200(4):493-505.
20. Hare KJ, Wilkinson RW, Jenkinson EJ, Anderson G. Identification of a developmentally regulated phase of postselection expansion driven by thymic epithelium. *J Immunol*. 1998;160(8):3666-3672.
21. Kurobe H, Liu C, Ueno T, et al. CCR7-dependent cortex-to-medulla migration of positively selected thymocytes is essential for establishing central tolerance. *Immunity*. 2006;24(2):165-177.
22. Nitta T, Nitta S, Lei Y, Lipp M, Takahama Y. CCR7-mediated migration of developing thymocytes to the medulla is essential for negative selection to tissue-restricted antigens. *Proc Natl Acad Sci USA*. 2009;106(40):17129-17133.
23. Boursalian TE, Golob J, Soper DM, Cooper CJ, Fink PJ. Continued maturation of thymic emigrants in the periphery. *Nat Immunol*. 2004;5(4):418-425.
24. Cowan JE, Parnell SM, Nakamura K, et al. The thymic medulla is required for Foxp3+ regulatory but not conventional CD4+ thymocyte development. *J Exp Med*. 2013;210(4):675-681.
25. Nakano H, Mori S, Yonekawa H, Nariuchi H, Matsuzawa A, Kakiuchi T. A novel mutant gene involved in T-lymphocyte-specific homing into peripheral lymphoid organs on mouse chromosome 4. *Blood*. 1998;91(8):2886-2895.
26. Link A, Vogt TK, Favre S, et al. Fibroblastic reticular cells in lymph nodes regulate the homeostasis of naive T cells. *Nat Immunol*. 2007;8(11):1255-1265.
27. Kozai M, Kubo Y, Katakai T, et al. Essential role of CCL21 in establishment of central self-tolerance in T cells. *J Exp Med*. 2017;214(7):1925-1935.
28. Yu W, Nagaoka H, Jankovic M, et al. Continued RAG expression in late stages of B cell development and no apparent re-induction after immunization. *Nature*. 1999;400(6745):682-687.
29. Van Vliet E, Jenkinson EJ, Kingston R, Owen JJ, Van Ewijk W. Stromal cell types in the developing thymus of the normal and nude mouse embryo. *Eur J Immunol*. 1985;15(7):675-681.
30. Purvanov V, Matti C, Samson GPB, Kindinger I, Legler DF. Fluorescently tagged CCL19 and CCL21 to monitor CCR7 and ACKR4 functions. *Int J Mol Sci*. 2018;19(12):3876.
31. Nakano H, Gunn MD. Gene duplications at the chemokine locus on mouse chromosome 4: multiple strain-specific haplotypes and the deletion of secondary lymphoid-organ chemokine and EBI-1 ligand chemokine genes in the plt mutation. *J Immunol*. 2001;166(1):361-369.

32. Lo JC, Chin RK, Lee Y, et al. Differential regulation of CCL21 in lymphoid/nonlymphoid tissues for effectively attracting T cells to peripheral tissues. *J Clin Invest*. 2003;112(10):1495-1505.

33. White AJ, Baik S, Parnell SM, et al. A type 2 cytokine axis for thymus emigration. *J Exp Med*. 2017;214(8):2205-2216.

34. Schaeuble K, Britschgi MR, Scarpellino L, et al. Perivascular fibroblasts of the developing spleen act as LTα1β2-dependent precursors of both T and B zone organizer cells. *Cell Rep*. 2017;21(9):2500-2514.

35. Sitnik KM, Wendland K, Weishaupt H, et al. Context-dependent development of lymphoid stroma from adult CD34(+) adventitial progenitors. *Cell Rep*. 2016;14(10):2375-2388.

36. Bao X, Moseman EA, Saito H, et al. Endothelial heparan sulfate controls chemokine presentation in recruitment of lymphocytes and dendritic cells to lymph nodes [*Immunity*. 2011;34(5):820]. *Immunity*. 2010;33(5):817-829.

37. von Andrian UH, Mempel TR. Homing and cellular traffic in lymph nodes. *Nat Rev Immunol*. 2003;3(11):867-878.

38. de Paz JL, Moseman EA, Noti C, Polito L, von Andrian UH, Seeberger PH. Profiling heparin-chemokine interactions using synthetic tools. *ACS Chem Biol*. 2007;2(11):735-744.

39. Chappell D, Jacob M, Rehm M, et al. Heparinase selectively sheds heparan sulphate from the endothelial glycocalyx. *Biol Chem*. 2008;389(1):79-82.

40. Hovingh P, Linker A. The enzymatic degradation of heparin and heparitin sulfate. 3. Purification of a heparitinase and a heparinase from flavobacteria. *J Biol Chem*. 1970;245(22):6170-6175.

41. Lucas B, James KD, Cosway EJ, et al. Lymphotoxin β receptor controls T cell progenitor entry to the thymus. *J Immunol*. 2016;197(7):2665-2672.

42. Seach N, Ueno T, Fletcher AL, et al. The lymphotoxin pathway regulates Aire-independent expression of ectopic genes and chemokines in thymic stromal cells. *J Immunol*. 2008;180(8):5384-5392.

43. Cosway EJ, Ohigashi I, Schauble K, et al. Formation of the intrathymic dendritic cell pool requires CCL21-mediated recruitment of $CCR7^{+}$ progenitors to the thymus. *J Immunol*. 2018;201(2):516-523.

44. Zamora-Pineda J, Kumar A, Suh JH, Zhang M, Saba JD. Dendritic cell sphingosine-1-phosphate lyase regulates thymic egress. *J Exp Med*. 2016;213(12):2773-2791.

45. Liu C, Saito F, Liu Z, et al. Coordination between CCR7- and CCR9-mediated chemokine signals in prevascular fetal thymus colonization. *Blood*. 2006;108(8):2531-2539.

46. Krueger A, Willenzon S, Lyszkiewicz M, Kremmer E, Förster R. CC chemokine receptor 7 and 9 double-deficient hematopoietic progenitors are severely impaired in seeding the adult thymus. *Blood*. 2010;115(10):1906-1912.

47. Zlotoff DA, Sambandam A, Logan TD, Bell JJ, Schwarz BA, Bhandoola A. CCR7 and CCR9 together recruit hematopoietic progenitors to the adult thymus. *Blood*. 2010;115(10):1897-1905.

48. Misslitz A, Pabst O, Hintzen G, et al. Thymic T cell development and progenitor localization depend on CCR7. *J Exp Med*. 2004;200(4):481-491.

49. Cowan JE, McCarthy NI, Anderson G. CCR7 controls thymus recirculation, but not production and emigration, of Foxp3(+) T cells. *Cell Rep*. 2016;14(5):1041-1048.

50. Havran WL, Allison JP. Origin of Thy-1+ dendritic epidermal cells of adult mice from fetal thymic precursors. *Nature*. 1990;344(6261):68-70.

51. Parker ME, Ciofani M. Regulation of γδ T cell effector diversification in the thymus. *Front Immunol*. 2020;11:42.